Co-Sputtered Thin Film Consisting of Platinum Nanoparticles Embedded in Graphite-Like Carbon and Its High Electrocatalytic Properties for Electroanalysis

Tianyan You,[†] Osamu Niwa,*[,†] Tsutomu Horiuchi,[†] Masato Tomita,[†] Yuzuru Iwasaki,[†] Yuko Ueno,[†] and Shigeru Hirono[‡]

NTT Lifestyle and Environmental Technology Labs, 3-1 Morinosato, Wakamiya, Atsugi, Kanagawa 243-0198, Japan, and NTT Afty Corporation, 4-16-30 Shimorenjyaku, Mitaka, Tokyo 181-0013 Japan

Received June 5, 2002. Revised Manuscript Received September 26, 2002

The radio frequency (RF) sputtering method was used to prepare nanoscale platinum (0) particles highly dispersed in a graphite-like carbon film (Pt−NEGCF) by co-sputtering platinum and carbon. The preparation is very simple, controllable, and reproducible. We studied this film with respect to its structural characterization and electrocatalytic properties. The XPS spectrum reveals that the platinum state in the Pt−NEGCF is platinum (0). TEM images show that the structure of the carbon in the film is graphite-like and that the platinum particles are highly dispersed in the carbon matrix. The electrochemical properties of the Pt−NEGCF electrode were evaluated. Compared with Pt bulk electrode, this film electrode is highly electrocatalytic as regards hydrogen evolution, dioxygen reduction, and hydrogen peroxide oxidation with good stability.

Introduction

Highly dispersed nanoscale platinum particles have been attracting growing interest because of their unique physical and chemical properties, as well as with regard to their applications in catalysis,[1−12] magnetism,[13] electronics,[14,15] and fuel cells.[16−21] There are several methods for preparing metal clusters including chemical reduction,[22−24] photolysis,[25] microwave,[26−27] an electrochemical process,[28−32] metal evaporation,[33−36] gas-phase reduction,[37] and decomposition.[38−41] Most of the above methods can produce nanoparticles on a supported

* To whom correspondence should be addressed. Tel: +81-46-240-3517. Fax: +81-46-240-4728. E-mail: niwa@aecl.ntt.co.jp.
[†] NTT Lifestyle and Environmental Technology Labs.
[‡] NTT Afty Corporation.

(1) Davis, S. C.; Klabunde, K. J. *Chem. Rev.* **1982**, *82*, 153.
(2) Wang, S.-W.; Falicov, L. M.; Searcy, A. W. *Surf. Sci.* **1984**, *143*, 609.
(3) Stevenson, S. A.; Dumesic, J. A.; Baker, R. T. K.; Ruckenstein, E. *Metal-Support Interactions in Catalysis, Sintering, and Redispersion;* Van Nostrand Reinhold: New York, 1987.
(4) Pool, R. *Science* **1990**, *24*, 1186.
(5) Bernal, S.; Botana, F. J.; Calvino, J. J.; López-Cartes, C.; Pérez-Omil, J. A.; Rodríguez-Izquierdo, J. M. *Ultramicroscopy* **1998**, *72*, 135.
(6) Freelink, T.; Visscher, W.; van Veen, J. A. R. *J. Electroanal. Chem.* **1995**, *382*, 65.
(7) Takasu, Y.; Ohashi, N.; Zhang, X. G.; Murakami, Y.; Minagawa, H.; Sato, S.; Yahikozawa, K. *Electrochim. Acta* **1996**, *41*, 2595.
(8) Morris, C. A.; Anderson, M. L.; Stroud, R. M.; Merzbacher, C. I.; Rolison, D. R. *Science* **1999**, *284*, 622.
(9) Swider, K. E.; Rolison, D. R. *Langmuir* **1999**, *15*, 3302.
(10) Bernal, S.; Baker, R. T.; Burrows, A.; Calvino, J. J.; Kiely, C. J.; López-Cartes, C.; Pérez-Omil, J. A.; Rodríguez-Izquierdo, J. M. *Surf. Interface Anal.* **2000**, *29*, 411.
(11) Long, J. W.; Ayers, K. E.; Rolison, D. R. *J. Electroanal. Chem.* **2002**, *522*, 58.
(12) Tong, Y.; Rice, A.; Wieckowski, A.; Oldfield, E. *J. Am. Chem. Soc.* **2002**, *122*, 1123.
(13) Ziolo, R. F.; Giannelis, E. P.; Weinstein, B. A.; H'Horo, M. P.; Ganguly, B. N.; Mehrotra, V.; Russell, M. W.; Huffmann, D. R. *Science* **1992**, *257*, 219.
(14) Simon, U.; Schön, G.; Schmid, G. *Angew. Chem.*; *Int. Ed Engl.* **1993**, *32*, 250.
(15) Rueckes, T.; Kim, K.; Joselevich, E.; Tseng, G. Y.; Cheung, C.-L.; Lieber, C. M. *Science* **2000**, *289*, 94.
(16) Sattler, K.; Ross, P. N. *Ultramicroscopy* **1986**, *20*, 21.
(17) Watanabe, M.; Saegusa, S.; Stonehart, P. *Chem. Lett.* **1988**, 1487.
(18) Kinoshita, K. *J. Electrochem. Soc.* **1990**, *137*, 845. Hogarth, M. P.; Hards, G. A. *Platinum Met. Rev.* **1996**, *40*, 150.
(19) Kordesch, K.; Simader, G. *Fuel Cells and Their Applications.* VCH: Weinheim, Germany, 1996.
(20) Rolison, D. R.; Hagans, P. L.; Swider, K. E.; Long, J. W. *Langmuir* **1999**, *15*, 774.
(21) Long, J. W.; Sroud, R. M.; Swider-Lyons, K. E.; Rolison, D. R. *J. Phys. Chem. B.* **2000**, *104*, 9772.
(22) Turkevich, J.; Kim, G. *Science* **1970**, *169*, 873.
(23) Lewis, L. N.; Lewis, N. *J. Am. Chem. Soc.* **1986**, *108*, 7288.
(24) Yu, W.; Wang, Y.; Liu, H.; Zheng, W. *J. Mol. Catal., A: Chem.* **1996**, *112*, 105.
(25) Torigoe, K.; Esumi, K. *Langmuir* **1993**, *9*, 1664.
(26) Tu, W.; Liu, H. *Chem. Mater.* **2000**, *12*, 564.
(27) Yu, W.; Tu, W.; Liu, H. *Langmuir* **1999**, *15*, 6.
(28) Bruce, J. A.; Murahashi, T.; Wrighton, M. S. *J. Phys. Chem.* **1982**, *86*, 1552.
(29) Kao, W.-H.; Kuwana, T. *J. Am. Chem. Soc.* **1984**, *106*, 473.
(30) Itaya, K.; Takahashi, H.; Uchida, I. *J. Electroanal. Chem.* **1986**, *208*, 373.
(31) Reetz, M. T.; Helbig, W. *J. Am. Chem. Soc.* **1994**, *116*, 7401.
(32) Zoval, J. V.; Gorer, J. L.; Penner, R. M. *J. Phys. Chem. B* **1998**, *102*, 1166.
(33) Gillet, M.; Renou, A. *Surf. Sci.* **1979**, *90*, 91.
(34) Bowles, R. S.; Kolstad, J. J.; Calo, J. M.; Andres, R. P. *Surf. Sci.* **1981**, *106*, 117.
(35) Klabunde, K. J.; Li, Y.-X.; Tan, B.-J. *Chem. Mater.* **1991**, *3*, 30.
(36) Röder, H.; Hahn, E.; Brune, H.; Bucher, J.-P.; Kern, K. *Nature* **1993**, *366*, 141.
(37) Bartholomew, C. H.; Boudart, M. *J. Catal.* **1972**, *25*, 173.
(38) Esumi, K.; Tano, T.; Torigoe, K.; Meguro, K. *Chem. Mater.* **1990**, *2*, 564.
(39) Bradley, J. S.; Hill, E. W.; Klein, C.; Chaudret, B.; Duteil, A. *Chem. Mater.* **1993**, *5*, 254.
(40) Suslick, K. S.; Choe, S.-B.; Cichowlas, A. A.; Grinstaff, M. W. *Nature* **1991**, *353*, 414.
(41) Suslick, K. S.; Fang, M.; Hyeon, T. *J. Am. Chem. Soc.* **1996**, *118*, 11960.

10.1021/cm020636k CCC: $22.00
Published on Web 10/24/2002

surface or colloidal dispersions. However, very few papers have reported the preparation of uniform platinum-cluster dispersed carbon film. McCreery and coworkers[42−45] and others[46] have published a series of articles on the synthesis of nanoscale platinum (0) clusters in glassy carbon (not solely on a glassy carbon surface) by incorporation of platinum in a glassy carbon precursor followed by thermolysis at 600 °C. This kind of platinum (0) doped glassy carbon (Pt−GC) exhibits high catalytic activity for the reduction of H^+ and dioxygen. Joo et al.[47] synthesized a high dispersion of platinum nanoparticles supported on ordered nanoporous arrays of carbon. Here, we used a radio frequency (RF) method to form a graphite-like carbon film containing highly dispersed nanoscale platinum (0) particles by co-sputtering platinum and carbon. We studied this RF sputtered platinum-nanoparticles-embedded graphite-like carbon film (Pt−NEGCF) with respect to its structural characterization and electrocatalytic properties for reduction of H^+ and dioxygen, and the oxidation of hydrogen peroxide.

Experimental Section

Chemicals and Reagents. We purchased H_2O_2, H_2SO_4, and 0.1 M phosphate buffer solution (PBS, pH 7) from Kanto Chemical Co. Ltd. (Tokyo, Japan). We prepared a fresh concentration of H_2O_2 with 0.1 M PBS buffer (pH 7) from a 10 mM stock solution of H_2O_2 before every use. We purified the water used in the experiments with a Milli-Q system (Millipore, Bedford, MA). The polycrystalline Pt pellet and sintering carbon for sputtering were obtained from Tanaka Kikinzoku Co. (Japan).

Film Preparation. We prepared the Pt−NEGCF on a Si wafer by RF co-sputtering (ANELVA EP21, Japan) of carbon and Pt. The background pressure of the chamber was 1.0×10^{-7} Torr. The Ar gas pressure during sputtering was 1.0×10^{-2} Torr. The temperature of the Si substrate was controlled at 200 °C, and the RF power was 200 W. We can control the platinum contents (1−7%) by setting different numbers of Pt pellets on the carbon target to control the ratio of Pt/carbon surface area, without changing the sputtering parameters such as power and pressure. When the ratio of Pt/carbon surface area is 0.1, 0.35, and 0.7%, the Pt content in the Pt−NEGCF is 1.3, 2.9, and 6.5%, respectively. The film thickness was controlled to be 40 nm. Then, the wafer was cut into a rectangle and a plastic tape (with a 3-mm diameter hole) was fixed to it to form a Pt−NEGCF disk electrode.

Apparatus. We carried out cyclic voltammetry with an ALS/CHI 802 electrochemical analyzer (CH Instruments, Inc., Austin, TX) in a Faraday cage with a Pt−NEGCF (or Pt-bulk) working electrode ($d = 3$ mm), an Ag/AgCl (3 M KCl) reference electrode, and a platinum auxiliary electrode.

We performed flow injection analysis (FIA) experiments with an ALS/CHI 802 electrochemical analyzer (CH Instruments), a column oven CA-202, SER 300H608 (BAS, Japan), and a thin-layer radial flow cell (BAS, West Lafayette, IN). We undertook comparison experiments with Pt-bulk and Pt−NEGCF electrodes for both the CV and FIA measurements.

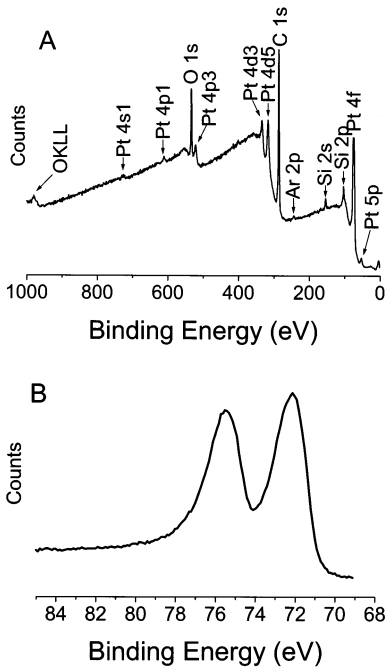

Figure 1. XPS spectrum of 2.9% Pt−NEGCF (A) and high-resolution spectrum of Pt(4f) line (B).

We observed the film, after peeling it from the silicon substrate, using a TEM apparatus (H-9000UHR, Hitachi Ltd., Japan) with an acceleration voltage of 200 kV.

X-ray photoelectron spectroscopy (XPS) was conducted at the NTT-AT Analysis Center with a Kratos AXIS Ultra (AlKα 1846.6 eV) spectrometer to determine the elemental composition of the film surface.

The conductivity of the Pt−NEGCF was measured with the conventional four-terminal method at room temperature.

Results and Discussion

Film Characterization. Figure 1A shows a typical XPS spectrum of Pt−NEGCF, which reveals that there is 2.9 at. % of platinum in the Pt−NEGCF. The C(1s) is used as an internal reference (284.6 eV). The binding energies of Pt($4f_{7/2}$) and Pt($4f_{5/2}$) electrons in the high-resolution spectrum of the Pt(4f) line (as shown in Figure 1B) are 72.1 and 75.5 eV, respectively, which indicates that the platinum state in the Pt−NEGCF is platinum (0). The slightly higher binding energy (∼1.0 eV) than that of bulk polycrystalline platinum may be due to the size-effect of small particle.[48−50]

Figure 2A shows a transmission electron micrograph (TEM) of a Pt−NEGCF front view. The dark spots and light features correspond to platinum nanoparticles and carbon matrix, respectively. We can observe that the matrix carbon in the Pt−NEGCF has small crystalline structures. The lattice images of the carbon with 3.6 Å spacing (wider than the ideal graphite crystal) were also obtained, which indicates that the carbon matrix is not amorphous, but disordered graphite-like.[53−55] Figure 2B

(42) Callstrom, M. R.; Neenan, T. X.; McCreery, R. L.; Alsmeyer, D. C. *J. Am. Chem. Soc.* **1990**, *112*, 4954.
(43) Pocard, N. L.; Alsmeyer, D. C.; McCreery, R. L.; Neenan, T. X.; Callstrom, M. R. *J. Am. Chem. Soc.* **1992**, *114*, 769.
(44) Pocard, N. L.; Alsmeyer, D. C.; McCreery, R. L.; Neenan, T. X.; Callstrom, M. R. *J. Mater. Chem.* **1992**, *2*, 771.
(45) Howard, H. D.; Pocard, N. L.; Alsmeyer, D. C.; Schueller, O. J. A.; Spontak, R. J.; Huston, M. E.; Huang, W.; McCreery, R. L.; Neenan, T. X.; Callstrom, M. R. *Chem. Mater.* **1993**, *5*, 1727.
(46) Schueller, O. J. A.; Pocard, N. L.; Huston, M. E.; Spontak, R. J.; Neenan, T. X.; Callstrom, M. R. *Chem. Mater.* **1993**, *5*, 11.
(47) Joo, S. H.; Chol, S. J.; Oh, I.; Kwak, J.; Liu, Z.; Terasaki, O.; Ryoo, R. *Nature* **2001**, *412*, 169.
(48) Takasu, Y.; Unwin, R.; Tesche, B.; Bradshaw, A. M.; Grunze, M. *Surf. Sci.* **1978**, *77*, 219.
(49) Kim, K. S.; Winograd, N. *Chem. Phys. Lett.* **1975**, *30*, 91.
(50) Eberhardt, W.; Fayet, P.; Cox, D.; Fu, Z.; Kaldor, A.; Sherwood, R.; Sondericker, D. *Phys. Scr.* **1990**, *41*, 892.
(51) Robertson, J. *Adv. Phys.* **1986**, *35*, 317.
(52) Takasu, Y.; Fujii, Y.; Yasuda, K.; Iwanaga, Y.; Matsuda, Y. *Electrochim. Acta* **1989**, *34*, 453.
(53) McCreery, R. L. In *Electroanalytical Chemistry*, Vol. 17; Bard, A. J., Ed.; Marcel Dekker: New York, 1991, p 221.

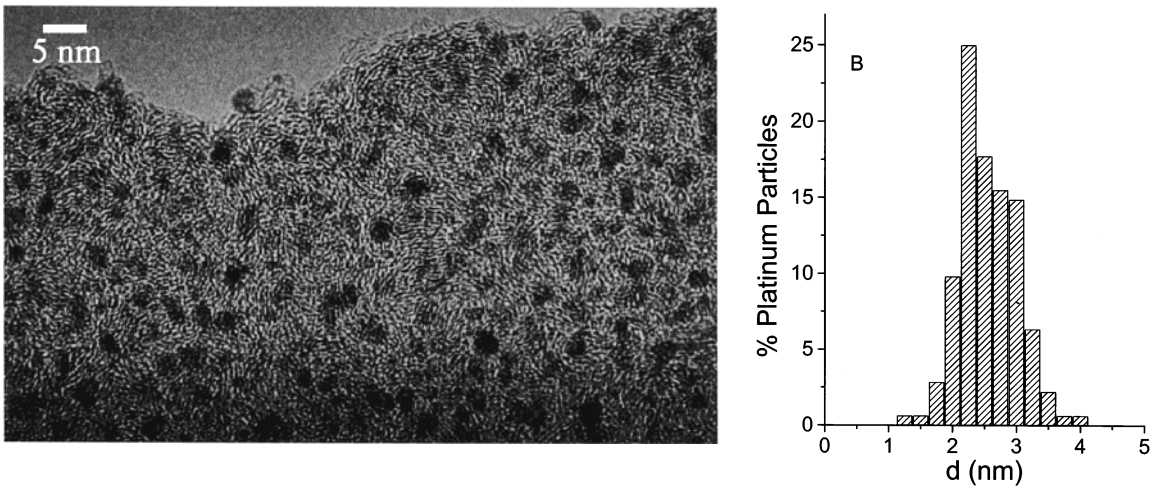

Figure 2. Transmission electron micrograph (TEM) image (A) and histogram of the platinum size distribution (B) of the 2.9% Pt−NEGCF.

illustrates the histogram of the platinum particle size distribution of 2.9% Pt−NEGCE. We measured 300 particles to study the platinum nanoparticle distribution. Figure 2A shows only a part of the TEM image area investigated for Figure 2B. The distribution of the platinum particles varies between 1 and 4 nm. Moreover, about 83% of the Pt particles sizes are in a narrow range from 2 to 3 nm. The average diameter of the platinum particle size is ∼2.5 nm. This means that the RF sputtering method is a potential way to prepare narrow distribution of platinum particles. The platinum particles in 2.9% Pt−NEGCF are nanoscale in size and highly dispersed in the graphite-like carbon film. The lattice spacing of the Pt−NEGCF measured by electron diffraction Pt(111) is 2.265 Å, which is in good agreement with the theoretical value for polycrystalline platinum. The side view of Pt−NEGCF was also studied by TEM measurements. We obtained the lattice spacing for carbon and Pt (111), 3.65 and 2.265 Å, respectively, which coincides with those for the front view.

We also carried out TEM measurements for 1.3% and 6.5% Pt−NEGCFs. The average particle size obtained for the two different Pt atom concentration Pt−NEGCFs is about 2.5 nm, same as that of 2.9% Pt−NEGCF. The variation of Pt content does not change the Pt nanoparticles size. This is different from the previous works,[42−46] which show that the Pt particles sizes increase with the higher Pt atom concentration. They prepared 0.9, 1.1, and 1.5% Pt-GCs, with the average cluster sizes of 8, 10, and 15 Å, respectively. The RF sputtering method has the advantage to form different Pt content Pt−NEGCFs with the same average particle size.

We measured the conductivity of both a RF carbon film and 2.9% Pt−NEGCF. The conductivity of the RF carbon film is 24 $S \cdot cm^{-1}$. This value is much higher than that for amorphous carbon film ($\sim 10^{-2}$ S/cm)[51] because the graphite-like structure was observed in Pt−NEGCF as shown in Figure 2A. After co-sputtering with platinum, the film conductivity increases to 103 $S \cdot cm^{-1}$ due to the highly dispersed platinum in the carbon film.

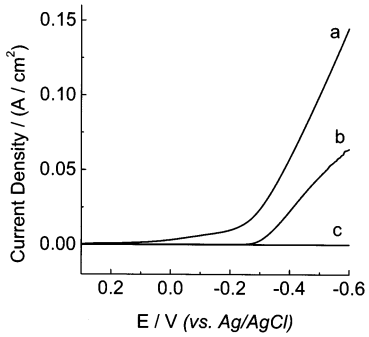

Figure 3. Hydrogen evolution obtained in 0.05 M H_2SO_4 at 2.9% Pt−NEGCF (a), Pt-bulk (b), and GC (c) electrodes, respectively. Scan rate, 50 mV/s.

Because RF carbon film is conductive, the Pt−NEGCF electrode works as a platinum nano-array electrode.

Electrochemistry of the Pt−NEGCF Electrode. We studied the electrochemical properties of 1.3, 2.9, and 6.5% Pt−NEGCFs electrodes for H^+ reduction, dioxygen reduction, and electrooxidation of hydrogen peroxide. Because the 2.9% Pt−NEGCF electrode exhibited the highest current density among the three different film electrodes, it was used for this work.

We evaluated the electrocatalytic ability of 2.9% Pt−NEGCF (Figure 3a) with respect to H^+ reduction in 0.05 M sulfuric acid compared with Pt-bulk (Figure 3b) and GC (Figure 3c) electrodes. Before the experiments, we polished the Pt-bulk electrode and scanned it in sulfuric acid until we obtained cyclic voltammogram (CV) characteristics indicating a clean Pt electrode. As shown in Figure 3, the current density value of H^+ reduction at the Pt−NEGCF electrode is much higher than that obtained at the Pt-bulk electrode. The exchange current density increases as the platinum particle size decreases.[52] In addition, the current at the Pt−NEGCF electrode does not decay as quickly as that at a Pt-bulk electrode. The current density at the Pt−NEGCF electrode decreased 25% after 2 h scanning, whereas it decreased about 80% at the Pt-bulk electrode. Moreover, the hydrogen evolution potential became positive as the platinum particle size decreased.

Figure 4 shows CVs of dioxygen reduction at the 2.9% Pt−NEGCF (Figure 4a), Pt-bulk (Figure 4b), and GC (Figure 4c) electrodes. The results show that electro-

(54) Hayashi, T.; Hirono, S.; Tomita, M.; Umemura, S. *Nature* **1996**, *381*, 772.
(55) Babonneau, D.; Cabioc'h, T.; Naudon, A.; Girard, J. C.; Denanot, M. F. *Surf. Sci.* **1998**, *409*, 358.

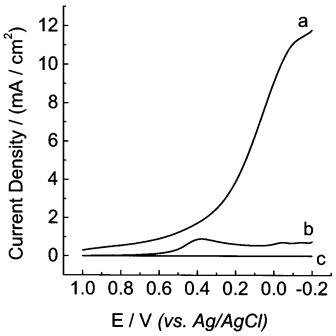

Figure 4. Electroreduction of saturated dioxygen in 0.5 M H_2SO_4 at 2.9% Pt−NEGCF (a), Pt-bulk (b), and GC (c) electrodes, respectively. Scan rate, 50 mV/s.

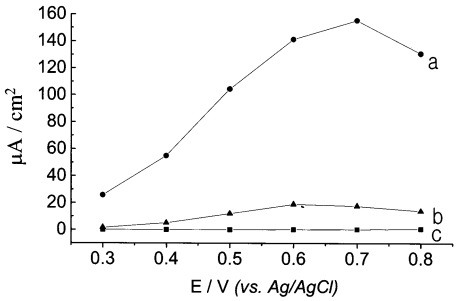

Figure 5. Hydrodynamic voltammograms of 100 μM hydrogen peroxide at 2.9% Pt−NEGCF (a), Pt-bulk (b), and GC (c) electrodes. Sample injection, 20 μL; run buffer, 0.1 M PBS, pH 7; flow rate, 0.5 mL/min.

catalytic activity of Pt−NEGCF as regards dioxygen reduction is much higher than that of the Pt-bulk electrode. In addition, the reduction potential is at about 0 V, which is about 0.4 V lower than that obtained at the Pt-bulk electrode. Compared with the Pt-bulk electrode, the Pt−NEGCF electrode has advantages in terms of dioxygen reduction with both a high current density and a comparatively low potential, which may make it useful as a potential electrode material for a dioxygen consumption measurement type biosensor.

We also studied the CVs for hydrogen peroxide oxidation at a 2.9% Pt−NEGCF electrode to evaluate its properties as an electrode for bio-electroanalytical chemistry. This is because the product of commonly used oxidase enzymes (such as glucose and lactate oxidases) is hydrogen peroxide. The oxidation peak potential was ~0.57 V at the Pt−NEGCF electrode, which is 70 mV lower than that at the Pt-bulk electrode (not shown).

Figure 5a shows hydrodynamic voltammograms (HDVs) for hydrogen peroxide at the 2.9% Pt−NEGCF electrode in the thin layer radial flow cell obtained by flow injection analysis (FIA). The responses of the Pt-bulk and GC electrodes were also measured for comparison. It can be seen that the current density at the GC electrode is very low because of its high overpotential for hydrogen peroxide oxidation. In contrast, we obtained a very high electrocatalytic current density at the 2.9% Pt−NEGCF electrode, which was 10 times higher than that obtained at the Pt-bulk electrode. The lower oxidation potential and higher current density at the Pt−NEGCF electrode reveals its high electrocatalytic ability with regard to the electrooxidation of hydrogen peroxide. The Pt−NEGCF electrode was also very stable during the FIA measurements. The response was linear between 2 μM and 5 mM. The film electrode has a very high sensitivity for the electrooxidation of H_2O_2. A limit of detection of 0.01 μM was determined ($S/N = 3$). The reproducibility of the peak current response for 100 μM H_2O_2 at the Pt−NEGCF electrode was also studied. The current response changes very little for continuous measurements of H_2O_2. The relative standard deviation was found to be 1.5% ($n = 6$). The successful detection of H_2O_2 at the Pt−NEGCF electrode in both stationary and flow systems indicate that this film is a potential electrode material for a H_2O_2-based biosensor application.

In comparison with methods reported in prior work,[42−46] the RF method is relatively simple. We can prepare Pt−NEGCF at the low temperature of 200 °C, whereas prior work required a higher temperature of 600 °C. The Pt−NEGCF electrode has highly electrocatalytic responses for hydrogen evolution and dioxygen reduction with good stability, which is similar to the references.[42−45] In addition, we used the Pt−NEGCF electrode for the electrooxidation of H_2O_2 in a flow system with a high sensitivity and good reproducibility, which indicates that this film electrode is a potential material for practical electroanalysis.

Conclusion

We employed an RF sputtering method for preparing nanoscale platinum (0) clusters in conductive graphite-like carbon film. The preparation is very simple, controllable, and reproducible. We can prepare Pt−NEGCF with different controlled platinum atom concentrations (1−7%). The Pt−NEGCF electrode has high activity and good stability for hydrogen evolution and dioxygen reduction. Moreover, this electrode is suitable for measuring hydrogen peroxide because of its extremely high electrocatalytic oxidation ability with excellent stability, which is important for biosensing applications.

CM020636K